KSME Journal, Vol. 3, No. 2, pp. 121~129, 1989.

STRESS FIELD NEAR TRANSVERSE CRACKS UNDER EXTENSION OR IN-PLANE SHEAR IN CROSS-PLY COMPOSITE LAMINATES

S. Im* and T.W. Kim*

(Received July 20, 1989)

Based upon the method of eigenfunction expansion and Leknitskii's complex-variable potentials for the generalized plane deformaion, the singular stress field near transverse cracks is examined for cross-ply composite laminates under two types of deformation, extension and in-plane shear. The stress singularity for each deformation is obtained from the eigenvalue equation resulting from appropriate near field conditions. It is found that the stress singularity for in-plane shear deformation is much stronger than for extension. To compute the stress intensity, use is made of the asymptotic representation for the stress and displacement field in conjunction with the singular hybrid finite element method. The numerical results are confirmed through comparison to those from other numerical techniques such as the boundary collocation method.

Key Words: Eigenvalues, Stress Singularity, Composite Laminates, Transverse Cracks, Cross-Ply, Hybrid Finite Element Method

1. INTRODUCTION

Recently, the rapid increase in applications of advanced fiber composite laminates to many engineering structures and components has led to significant efforts in research on the mechanics of composite laminates. One of the important problems that has received an increasing attention in the mechanics of composite laminates is how to deal with local deformation and complex stresses near geometric discontinuities and structural defects, such as edges, cutouts, cracks, and re-entrant corners, which are prevalent in almost all of the advanced composite materials and structures owing to fabrication and joining requirements as well as design considerations. Generally, the difficulties involve local stress singularities and inherently three-dimensional state of complex stresses. Moreover, the high local stresses and associated deformations caused by these structural and material discontinuities always result in undesirable delamination and transverse crack initiation and growth, leading to the final fracture. Thus, this class of mechanics problems has been of significant interest to researchers in mechanics of materials.

For an anisotropic composite body, several authors reported the stress singularities and stress distributions near the free edge in composite laminates(see Wang and Choi, 1982; Zwier, Ting and Spilker, 1982; Ting and Chou, 1981). The problems of delamination cracks in an anisotropic composite laminate were treated, in the same way as the free edge problems, by Wang(1984), and Wang and Choi(1983). The stress singularity near the transverse cracks in anisotropic composite laminates was first reported by Ting and Hoang(1984) although the solutions to the similar problems were reported for isotropic bi-materials somewhat earlier(see, for example, Zak and Williams, 1963; Bogy, 1971; Cook and Erdogan, 1972). Recently Im(1989) reduced, by exploiting the material symmetry, the algebra involved in calculating the stress singularity near transverse cracks in anisotropic composite laminates, and computed the stress intensity near the crack tip using the boundary collocation method.

The purpose of the present work is to examine the singular stress field near the transverse cracks in a cross-ply laminate, with the aid of singular hybrid finite element method combined with the asymptotic solution for stress and displacement near the crack tip. It is assumed that the transverse cracks, occurring in 90° ply and terminating perpendicularly to the ply interface, are arranged with a uniform spacing. The asymptotic solution is then obtained, under the assumption of the generalized plane deformation, from Lekhnitskii's complex potentials and the eigenfunction expansion; the system of coupled governing partial differential equations is solved using the general solution in the form of complex variable potential functions and its series expansion, and appropriate near field conditions are imposed to lead to the eigenvalue equations, which determine the structures of the asymptotic solutions, including the stress singularity. The asymptotic solutions, determined within the unknown constants, is then incorporated into a singular crack-tip finite element, which is combined with the regular finite elements to complete the solution.

The numerical results are confirmed, in terms of the stress intensity, through comparison to those obtained from the boundary collocation technique. The characteristics of the singular stress field near the crack tip is briefly discussed for the aforementioned two types of deformations, extension(or stretching) and in-plane shear.

*Department of Mechanical Engineering, Korea Advanced Institute of Science and Technology, P.O. Box 150, Cheonryang Seoul 130-650, Korea

2. DEFORMATION OF A CROSS-PLY COMPOSITE LAMINATE WITH TRANSVERSE CRACKS

2.1 Statement of the Problem and Basic Equations

Consider the two types of cross-ply composite laminate, $[90/0]_s$ and $[0/90]_s$ subjected to extension or in-plane shear, respectively. As the load increases, there will occur numerous transverse cracks running parallel to the fiber orientation of the 90° ply, with an approximately uniform spacing along the length of the laminates. In most cases, the transverse cracks, occurring in the 90° ply, terminate perpendicularly to the ply interface. To simplify the problem, we assume that the cracks are uniformly arranged with the configuration symmetric about the mid-plane, as shown in Fig. 1, so that the overall arrangement is obtained by repetition of the unit cell(Fig. 1).

We take a rectangular Cartesian coordinate system with origin at one of the crack tips. We choose the x axis to be along the length of composite laminates while the y axis is taken to be along the direction of the laminate thickness, and then the z axis becomes along the laminate width, which is parallel to the cracks(see Fig. 1).

As stated earlier, we consider two types of deformations separately, extension along the x axis and in-plane shear on the x-z plane(anti-plane shear on the x-y plane). In addition, we assume that the laminate dimension in the z direction(laminate width) is sufficiently large compared with the laminate thickness and that the state of deformation remains the same on every section parallel to the x-y plane, so that the composite laminate is in the state of the generalized plane deformation, in which the state of deformation is not dependent upon the z coordinate.

According to Lekhnitskii(1963), the state of stress for the generalized plane deformation in the absence of body forces can be represented by the two stress potentials $F(x, y)$ and $\Psi(x, y)$:

$$\begin{aligned}
&\sigma_{xx}=\sigma_1=\frac{\partial^2 F}{\partial y^2},\quad \sigma_{yy}=\sigma_2=\frac{\partial^2 F}{\partial x^2},\\
&\sigma_{xy}=\sigma_6=\frac{-\partial^2 F}{\partial x\partial y},\quad \sigma_{xz}=\sigma_5=\frac{\partial \Psi}{\partial y},\\
&\sigma_{yz}=\sigma_4=\frac{-\partial \Psi}{\partial x}
\end{aligned}\tag{1}$$

Hereafter the contracted notation σ_i will be used, whenever convenient, in place of the notation σ_{xx}, σ_{yy}, σ_{zz}, σ_{yz}, σ_{xz}, σ_{xy}. From the constitutive equations and compatibility relation the stress component σ_{zz} and the displacement component $u_i(u, v, w)$ may be given as in Wang and Choi(1982) :

$$\begin{aligned}
&\sigma_{zz}=(A_1x+A_2y+A_3)/S_{33}-\frac{S_{i3}}{S_{33}}\sigma_i,\quad (i=1, 2, 4, 5, 6)\\
&u_1=-A_1z^2/2-A_4yz+U(x, y)\\
&u_2=-A_2z^2/2+A_4xz+V(x, y)\\
&u_3=(A_1x^2+A_2y+A_3)z+W(x, y)
\end{aligned}\tag{2}$$

where A_1, A_2, A_3 and A_4 are constants related to bending in the x-z and y-z planes and axial extension along the z-axis and torsion along the z-axis, respectively ; S_{ij} is the compliance tensor in generalized Hooke's law for each lamina in the contracted notation,

$$\varepsilon_i=S_{ij}\sigma_j\ (i, j=1, 2, 3, \cdots, 6)\tag{3}$$

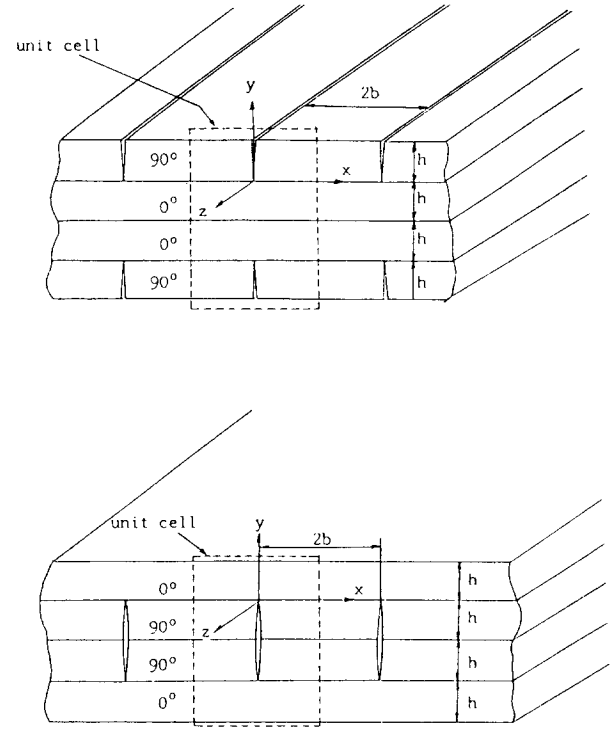

Fig. 1 Transverse cracks in $[90°/0°]_s$ and $[0°/90°]_s$

The engineering strains in equation (3) are defined in a Cartesian coordinated system by

$$\begin{aligned}
&\varepsilon_1=\varepsilon_x=\frac{\partial u}{\partial x},\quad \varepsilon_2=\varepsilon_y=\frac{\partial v}{\partial y},\\
&\varepsilon_3=\varepsilon_z=\frac{\partial w}{\partial z},\quad \varepsilon_4=\varepsilon_{yz}=\frac{\partial v}{\partial z}+\frac{\partial w}{\partial y}\\
&\varepsilon_5=\gamma_{zx}=\frac{\partial u}{\partial z}+\frac{\partial w}{\partial x},\quad \varepsilon_6=\gamma_{xy}=\frac{\partial u}{\partial y}+\frac{\partial v}{\partial x}
\end{aligned}$$

By using the Lekhnitskii stress functions and following the procedure given in Leknitskii(1963), a system of coupled governing partial differential equations for the boundary-layer field in a composite laminate is obtained as

$$L_3F+L_2\Psi=-2A_4+A_1S_{34}/S_{33}-A_2S_{35}/S_{33}\tag{4.a}$$
$$L_4F+L_3\Psi=0,\tag{4.b}$$

where L_2, L_3 and L_4 are linear differential operators of the second, third and fourth orders defined by

$$\begin{aligned}
L_2&=\bar{S}_{44}\frac{\partial^2}{\partial x^2}-2\bar{S}_{45}\frac{\partial^2}{\partial x\partial y}+\bar{S}_{55}\frac{\partial^2}{\partial y^2}\\
L_3&=-\bar{S}_{24}\frac{\partial^3}{\partial x^3}+(\bar{S}_{25}+\bar{S}_{46})\frac{\partial^3}{\partial x^2\partial y}\\
&\quad-(\bar{S}_{14}+\bar{S}_{56})\frac{\partial^3}{\partial x\partial y^2}+\bar{S}_{15}\frac{\partial^3}{\partial y^3}\\
L_4&=\bar{S}_{22}\frac{\partial^4}{\partial x^4}-2\bar{S}_{26}\frac{\partial^4}{\partial x^3\partial y}\\
&\quad+(2\bar{S}_{12}+\bar{S}_{66})\frac{\partial^4}{\partial x^2\partial y^2}-2\bar{S}_{16}\frac{\partial^4}{\partial x\partial y^3}+\bar{S}_{11}\frac{\partial^4}{\partial y^4},
\end{aligned}\tag{5.a}$$

in which $\bar{S}_{ij}$ are the reduced compliance tensor for each lamina, given as

$$\bar{S}_{ij}=S_{ij}-S_{i3}S_{3j}/S_{33} \quad (i,j=1,2,4,5,6) \tag{5.b}$$

For the cross-ply laminates under the present consideration, the coordinate axes are coincident with the principal directions of each lamina, and the coupled partial differential equations (4.a, b) are reduced to the decoupled forms,

$$L_4F=0,\ L_2\Psi=-2A_4, \tag{6.a, b}$$

where L_2 and L_4 are given by equation (5.a) with $S_{16}=S_{26}=S_{45}=0$ owing to the material symmetry. It is noted that the extension along the x axis now involves the function $F(x,y)$ and the displacement components u, v: on the other hand the shear in the x-z plane the function $\Psi(x,y)$ and the displacement component w alone. We can therefore consider the two equations (6.a, b) separately. It is emphasized here that the above equations should hold on each ply of the laminates.

The general solutions of equations (6.a, b) consist of the homogeneous solution and the particular solution that depends upon the loading parameters A_i. For the present problems, however, the loading parameters A_i are identically zero and the particular solution disappears for both of the two cases. The form of homogeneous solution is determined from the characteristics of the elliptic partial differential equations (6.a, b) on the complex plane:

$$z_k^{(\alpha)}=x+\mu_k^{(\alpha)}y,\ z_{k+2}^{(\alpha)}=\bar{z}_k^{(\alpha)},\ k=1,2,\ \alpha=1,2 \tag{7.a}$$

for equation (6.a), and

$$\begin{aligned} z_1^{(\alpha)}&=x+\xi_1^{(\alpha)}y \\ z_2^{(\alpha)}&=x+\xi_2^{(\alpha)}y=\bar{z}_1^{(\alpha)},\ \alpha=1,2 \end{aligned} \tag{7.b}$$

for equation (6.b), where $\alpha=1,2$ indicate the upper and lower materials, respectively, and $\mu_k^{(\alpha)}$ and $\xi_k^{(\alpha)}$ are the solution of the following polynomial equations

$$\bar{S}_{11}^{(\alpha)}\mu^4+(2\bar{S}_{12}^{(\alpha)}+\bar{S}_{66}^{(\alpha)})\mu^2+\bar{S}_{22}^{(\alpha)}=0,\ \bar{S}_{55}^{(\alpha)}\xi^2+\bar{S}_{44}^{(\alpha)}=0$$

In these equations the superscript (α) in μ and ξ has been omitted for simplicity, this will be omitted whenever there is no confusion. The homogeneous solution then takes the form for each ply.

$$F(x,y)=\sum_{k=1}^{4}F_k(z_k),\ \Psi(x,y)=\sum_{k=1}^{2}\Psi_k(\xi_k) \tag{8.a, b}$$

We seek for the asymptotic solution near the crack tip, which meets the near-field conditions-the traction free conditions on the crack surfaces and the continuity condition along the ply interface, and then we incorporate this solution into a special hybrid finite element, which can be combined with the regular displacement based finite element method to complete the solution.

2.2 The Near-Field Conditions

To obtain the asymptotic representation for the solution we need to consider the near-field conditions that the solution is required to meet near the crack tip. Assuming that the two plies are perfectly bonded along the interface, we can establish the continuity for traction and displacement along the interface. That is, for extension involving $F(x,y)$,

$$\sigma_{yy}^{(1)}=\sigma_{yy}^{(2)},\ \sigma_{xy}^{(1)}=\sigma_{xy}^{(2)},\ u^{(1)}=u^{(2)},\ v^{(1)}=v^{(2)}, \tag{9.a}$$

and for in-plane shear related to $\Psi(x,y)$,

$$\sigma_{yz}^{(1)}=\sigma_{yz}^{(2)},\ w^{(1)}=w^{(2)} \tag{9.b}$$

The traction free conditions on both of the crack surfaces, which the asymptotic solution is also required to satisfy exactly, are given as

$$\sigma_{xx}(0_+,y)=0,\ \sigma_{xy}(0_+,y)=0 \text{ on the } 90^\circ \text{ ply for } F(x,y), \tag{10.a}$$

and

$$\sigma_{xz}(0_+,y)=0 \quad \text{on the } 90^\circ \text{ ply for } \Psi(x,y), \tag{10.b}$$

where $x=0_+$ indicates the right crack surface. The above interface conditions and the traction free conditions should be considered also on the left region $x\le 0$. However, the advantage of symmetry can be taken so that the conditions on the region $x\le 0$ may be replaced by appropriate symmetry or antisymmetry conditions along the crack ligament (the undamaged part of the y axis). That is, we add

$$\begin{aligned} &u(x,y)=-u(-x,y),\ v(x,y)=v(-x,y) \quad \text{for } F \\ &\text{and } w(x,y)=-w(-x,y) \text{ for } \Psi, \end{aligned}$$

which can be recast into

$$\frac{\partial u(0_+,y)}{\partial y}=0,\ \frac{\partial v(0_+,y)}{\partial x}=0 \text{ for } F, \tag{11.a}$$

and

$$\frac{\partial w(0_+,y)}{\partial y}=0 \text{ for } \Psi \tag{11.b}$$

It is clear that we need only to consider the upper right part ($0\le x\le b,\ -h\le y\le h$) of the unit cell(Fig. 1), where h and b are the ply thickness and half the crack spacing, respectively. This is due to the material and geometric symmetry and the uniform spacing of the crack arrangement.

2.3 Asymptotic Representation for Stress and Displacement

In this section, we consider the asymptotic representation of the stress and displacement field near the crack tip, and with the aid of the foregiong conditions near the crack tip, we determine the sturcture of the asymptotic solution including the stress singularities. For clarity of presentation, we consider the extension and the in-plane shear, separately.

To determine the homogeneous solution(8.a) in the form of an asymptotic eigenfunction series, the following series expansion of power type for $F_k(z_k)$ is introduced

$$F_k(z_k)=\sum_{n=1}^{\infty}C_{kn}\frac{z_k^{\delta_n+2}}{(\delta_n+1)(\delta_n+2)}, \tag{12}$$

where δ_n and C_{kn} are the eigenvalues and the constants to be determined, respectively. Substituting equation (12) into equation (1), we obtain the homogeneous solution for the stress components

$$\sigma_{xx}=\sum_{n=1}^{\infty}\sum_{k=1}^{2}[C_{kn}\mu_k^2z_k^{\delta_n}+C_{(k+2)n}\bar{\mu}_k^2\bar{z}_k^{\delta_n}] \tag{13.a}$$

$$\sigma_{yy}=\sum_{n=1}^{\infty}\sum_{k=1}^{2}[C_{kn}z_k^{\delta n}+C_{(k+2)n}\bar{z}_k^{\delta n}] \tag{13.b}$$

$$\sigma_{xy}=-\sum_{n=1}^{\infty}\sum_{k=1}^{2}[C_{kn}\mu_k z_k^{\delta n}+C_{(k+2)n}\bar{\mu}_k\bar{z}_k^{\delta n}] \tag{13.c}$$

With the aid of the generalized Hook's law (3) and the strain-displacement relation, the associated displacemet components can be obtained as

$$u=\sum_{n=1}^{\infty}\Big[\sum_{k=1}^{2}\{C_{kn}p_k z_k^{\delta n+1}+C_{(k+2)n}\bar{p}_k\bar{z}_k^{\delta n+1}\}/(\delta_n+1)\Big], \tag{14.a}$$

$$v=\sum_{n=1}^{\infty}\Big[\sum_{k=1}^{2}\Big\{C_{kn}q_k z_k^{\delta n+1}+C_{(k+2)n}\bar{q}_k\bar{z}_k^{\delta n+1}\Big\}/(\delta_n+1)\Big], \tag{14.b}$$

where

$$p_k=\bar{S}_{11}\mu_k^2+\bar{S}_{12} \text{ and } q_k=\bar{S}_{12}\mu_k+\bar{S}_{22}/\mu_k$$

We add that the aforementioned representations (12) through (14.b) should be considered for each of the 90° and 0° ply.

The preceding homogeneous solution for the stress and displacement are required to satisfy the near-field conditions in Sec. 2.2. This then leads to a standard eigenvalue problem. Substituting the expressions for the stress and displacement (13.a) through (14.b) into the continuity conditions (9.a), the traction free conditions (10.a) and the symmetry conditions (11.a), we can establish the following 8 by 8 linear homogeneous equations in $C_{kn}^{(1)}$ and $C_{kn}^{(2)}$:

$$\Delta_{ij}^{(e)}(\delta_n)D_{jn}^{(e)}=0 \quad (i,j=1\sim 8), \tag{15}$$

where "(e)" indicates the extension and $D_{jn}^{(e)}=C_{jn}^{(1)}$, $D_{(j+4)n}^{(e)}=C_{jn}^{(2)}(j=1\sim 4)$ with the superscript (1), (2) denoting the upper and the lower ply, respectively. For the existence of nontrivial solution, the determinant of the coefficient matrix $\Delta_{ij}^{(e)}(\delta_n)$ should vanish,

$$|\Delta_{ij}^{(e)}(\delta_n)|=0, \tag{16}$$

which determines the eigenvalue δ_n. Once the eigenvalues are obtained, within unknown constants the eigenvectors $C_{kn}^{(\alpha)}(\alpha=1,2\ ;\ k=1\sim 4)$ can be found from equation (15). From the structure of $\Delta_{ij}^{(e)}(\delta_n)$, we can show that if δ_n is the root of the characteristic equation (16), so is its complex conjugate $\bar{\delta}_n$, so that the expressions for the stresses and displacements become real. For convenience, we take

$$C_{kn}^{(\alpha)}=\frac{1}{2}(\gamma_{1n}-i\gamma_{2n})b_{kn}^{(\alpha)} \quad \text{for complex } \delta_n,\ \mathrm{Im}[\delta_n]>0, \tag{17.a}$$

$$C_{kn}^{(\alpha)}=\frac{1}{2}\gamma_{3n}b_{kn}^{(\alpha)} \text{ for real } \delta_n, \tag{17.b}$$

when $b_{kn}^{(\alpha)}$ is the solution for $C_{kn}^{(\alpha)}$, computed from equation (15) by an approximate normalization, and γ_{1n}, γ_{2n}, γ_{3n} are constants to be determined to complete the solution. The asymptotic expressions for stress and displacement (13.a) through (14.b) are then written as

$$\sigma_i^{(\alpha)}=\sum_{n=1}^{\infty}P_{ni}^{(\alpha)} \quad (i=1,2,6) \tag{18.a}$$

$$u_j^{(\alpha)}=\sum_{n=1}^{\infty}Q_{nj}^{(\alpha)}, \quad (j=1,2) \tag{18.b}$$

where $P_{ni}^{(\alpha)}$ and $Q_{nj}^{(\alpha)}$ are given by

$$P_{ni}^{(\alpha)}=\gamma_{1n}Re[\phi_{in}]+\gamma_{2n}\ \mathrm{Im}\ [\phi_{in}] \tag{19.a}$$

$$\phi_{in}=\sum_{k=1}^{2}[b_{kn}^{(\alpha)}\Lambda_{ik}^{(\alpha)}z_k^{(\alpha)\delta n}+b_{(k+2)n}^{(\alpha)}\bar{\Lambda}_{ik}^{(\alpha)}\bar{z}_k^{(\alpha)\delta n}]$$

$$\Lambda_{1k}^{(\alpha)}=\mu_k^{(\alpha)2},\ \Lambda_{2k}^{(\alpha)}=1,\ \Lambda_{6k}^{(\alpha)}=-\mu_k^{(\alpha)},$$

if δ_n is complex, or

$$P_{ni}^{(\alpha)}=\gamma_{3n}Re\Big[\sum_{k=1}^{2}\{b_{kn}^{(\alpha)}\Lambda_{ik}^{(\alpha)}z_k^{(\alpha)\delta n}\}\Big] \text{ if } \delta_n \text{ is real,} \tag{19.b}$$

and

$$Q_{nj}^{(\alpha)}=\gamma_{1n}Re[\psi_{jn}]+\gamma_{2n}\ \mathrm{Im}\ [\psi_{jn}] \tag{20.a}$$

$$\psi_{jn}=\sum_{k=1}^{2}[b_{kn}^{(\alpha)}\Gamma_{jk}^{(\alpha)}z_k^{(\alpha)\delta n+1}+b_{(k+2)n}^{(\alpha)}\bar{\Gamma}_{jk}^{(\alpha)}\bar{z}_k^{(\alpha)\delta n+1}]/(\delta_n+1)$$

$$\Gamma_{1k}^{(\alpha)}=p_k^{(\alpha)},\ \Gamma_{2k}^{(\alpha)}=q_k^{(\alpha)}$$

if δ_n is complex, or

$$Q_{nj}^{(\alpha)}=\gamma_{3n}Re\Big[\sum_{k=1}^{2}b_{kn}^{(\alpha)}\Gamma_{jk}^{(\alpha)}z_k^{(\alpha)\delta n+1}/(\delta_n+1)\Big] \quad \text{if } \delta_n \text{ is real.} \tag{20.b}$$

For the in-plane shear deformation, we take

$$\Psi_k(z_k)=\sum_{n=1}^{\infty}C_{kn}\frac{z_k^{\delta n+1}}{(\delta_n+1)},$$

$$z_k=x+\xi_k y,\ k=1,2$$

Then the asymptotic homogeneous solution for the stress and displacement may be written as

$$\sigma_{yz}=-\sum_{n=1}^{\infty}(C_{1n}z_1^{\delta n}+C_{2n}\bar{z}_1^{\delta n}) \tag{21.a}$$

$$\sigma_{xz}=\sum_{n=1}^{\infty}(C_{1n}\xi_1 z_1^{\delta n}+C_{2n}\bar{\xi}_1\bar{z}_1^{\delta n}) \tag{21.b}$$

$$w=-S_{44}\sum_{n=1}^{\infty}(C_{1n}z_1^{\delta n+1}/\xi_1+C_{2n}\bar{z}_1^{\delta n+1}/\bar{\xi}_1)/(\delta_n+1) \tag{21.c}$$

As in the extension, we have so far omitted the superscript (α) indicating upper or lower ply. Substituting these representation into the near-field conditions (9.b), (10.b) and (11.b), we obtain the 4×4 linear equations is $C_{kn}^{(1)}$ and $C_{kn}^{(2)}$,

$$\Delta_{ij}^{(s)}(\delta_n)D_{jn}^{(s)}=0\ (i,j=1\sim 4) \tag{22.a}$$

$$D_{kn}^{(s)}=C_{kn}^{(1)},\ D_{(k+2)n}^{(s)}=C_{kn}^{(2)} \quad (k=1,2),$$

where the superscript (s) indicates the in-plane shear deformation on the $x-z$ plane. This leads to the characteristic equation

$$|\Delta_{ij}^{(s)}(\delta_n)|=0 \tag{22.b}$$

Introducing the real constants γ_{1n}, γ_{2n}, γ_{3n} as given by equations (17.a, b), we may write the asymptotic stress and displacement in the form of equations (18.a, b)

$$\sigma_i^{(\alpha)}=\sum_{n=1}^{\infty}P_{ni}^{(\alpha)}\ (i=4,5), \quad u_3=w=\sum_{n=1}^{\infty}Q_{n3}^{(\alpha)} \tag{23.a, b}$$

$$P_{ni}^{(a)}=\gamma_{1n}Re[\phi_{in}]+\gamma_{2n}\ \mathrm{Im}\ [\phi_{in}] \quad (24.a)$$
$$\phi_{in}=b_{1n}^{(a)}\Lambda_{i1}^{(a)}z_k^{(a)\delta_n}+b_{2n}^{(a)}\bar{\Lambda}_{i1}^{(a)}\bar{z}_k^{(a)\delta_n},$$
$$\Lambda_{41}^{(a)}=-1,\ \Lambda_{51}^{(a)}=\xi_1^{(a)}$$

if δ_n is complex, or

$$P_{ni}^{(a)}=\gamma_{3n}Re[b_{1n}^{(a)}\Lambda_{i1}^{(a)}z_k^{(a)\delta_n}] \text{ if } \delta_n \text{ is real,} \quad (24.b)$$

and

$$Q_{n3}^{(a)}=\gamma_{1n}Re[\psi_{3n}]+\gamma_{2n}\ \mathrm{Im}\ [\psi_{3n}] \quad (25.a)$$
$$\psi_{3n}=-(b_{1n}^{(a)}S_{44}^{(a)}z_1^{(a)\delta_n+1}/\xi_1^{(a)}+b_{2n}^{(a)}S_{44}^{(a)}\bar{z}_k^{(a)\delta_n+1}/\bar{\xi}_1^{(a)})/(\delta_n+1)$$

if δ_n is complex, or

$$Q_{n3}^{(a)}=-\gamma_{3n}Re[(b_{1n}^{(a)}S_{44}^{(a)}z_1^{(a)\delta_n+1}/\xi_1^{(a)}+b_{2n}^{(a)}S_{44}^{(a)}\bar{z}_k^{(a)\delta_n+1}/\bar{\xi}_1^{(a)})/(\delta_n+1)] \quad (25.b)$$

if δ_n is real.

The free constants γ_{1n}, γ_{2n}, γ_{3n} should be determined to match the far-field boundary conditions. For this we may use a numerical technique such as the boundary collocation method(Wang and Choi, 1982; Im, 1989), or the singular hybrid finite element method(Wang and Yuan, 1983), which will be discussed in the next section. For application of this numerical technique, a proper truncation of the eigenfunction series is needed, say $n=1\sim N$ in equations (18.a, b) and (23.a, b). These equations may then be put into the following forms

$$\sigma_i=\sum_{n=1}^{N}\beta_n f_i^n(x, y, \delta_n),$$
$$u_j=\sum_{n=1}^{N}\beta_n g_j^n(x, y, \delta_n) \quad (26.a, b)$$

where N is the number of the eigenvalues included for the two deformations (of course the number of the eigenvalues included may be different for the two deformations), and β_n denote the unknown free constants γ_{1n}, γ_{2n}, γ_{3n} for each deformation.

2.4 The Far-Field Conditions

The unknown constants β_n in equation (26.a, b) are to be determined such that they meet the remote boundary conditions at far-field. Due to the geometric and material symmetry, it is sufficient to consider only the upper right portion, as discussed earlier(see Fig. 1). Along the boundary of this portion, we examine the conditions for tractions or displacements. Consider first the extension in which every unit cell of length $2b$ is extended $2u_0$. On the crack surface at the left end, $x=0$, the traction free condition (10.a) hold; while neglecting the overall rigid translation we may fix the crack ligament and write the condition for the crack ligament,

$$u(0, y)=0,\ \sigma_{xy}(0, y)=0, \quad (27.a, b)$$

which is equivalent to the near-field condition (11.a). Note that the traction free condition (10.a) and the above conditions may be regarded as the far-field conditions away from the crack tip. On the other hand, at $x=b$ we have the uniform end displacement u_0 and the zero shear stress due to the symmetry

$$u(b, y)=u_0,\ \sigma_{xy}(b, y)=0,\ -h\le y\le h \quad (28.a, b)$$

On the top surface, the traction free conditions hold, so that

$$\sigma_{yy}(x, h)=\sigma_{xy}(x, h)=0,\quad 0\le x\le b \quad (29.a, b)$$

while, on the middle surface $y=-h$, symmetry condition gives

$$\sigma_{xy}(x, -h)=0,\ v(x, -h)=0,\quad 0\le x\le b \quad (30.a, b)$$

Next consider the in-plane shear deformation on the $x-z$ plane (the anti-plane shear deformation on the $x-y$ plane) in which every unit cell of length $2b$ is sheared by $2w_0$ in the z-direction. On the crack surface, we have the traction free condition (10.b). On the crack ligament and on the right end $x=b$, we may prescribe the displacement conditions,

$$w(0, y)=0\ (-h\le y\le 0),\ w(b, y)=w_0\ (-h\le y\le h) \quad (31.a, b)$$

while, on the top and the middle plane, we have the following traction free conditions

$$\sigma_{yz}(x, h)=0,\ \sigma_{yz}(x, -h)=0 \quad (32.a, b)$$

3. FINITE ELEMENT SOLUTION PROCEDURE

To complete the solution, we need to determine the unknown free constants γ_{1n}, γ_{2n}, γ_{3n} in the asymptotic representation for the stress and displacement such that it may meet the aforementioned far-field conditions. To match the asymptotic expressions with the far-field condition, we may use the boundary collocation technique(Wang and Choi, 1982), or the singular hybrid finite element method(Wang and Yuan, 1983). The boundary collocation technique was used to treat the case of extension in Im(1989). We here focus upon the singular hybrid finite element method to deal with each of the extension and the in-plane shear, and make a comparison of the results from the two approaches.

3.1 Formulation of the Singular Hybrid Element

In the singular hybrid finite element technique, the singular region around the crack tip is covered with a single hybrid element into which the asymptotic representation is incorporated, and the singular solution of the hybrid element is matched to the regular F.E.M solution of its surrounding. To construct the hybrid element, we begin with the hybrid variational functional $\Pi_{mh}(\boldsymbol{\sigma}, \boldsymbol{u}, \bar{\boldsymbol{u}})$ in Washizu(1982), which can be derived from the Reissner-Hellinger variational functional with a relaxed continuity condition along the interelement boundary with the aid of Lagrangian multiplier technique;

$$\Pi_{mh}(\boldsymbol{\sigma}, \boldsymbol{u}, \bar{\boldsymbol{u}})=\iint_{A_m}(\boldsymbol{\sigma}^T\ \boldsymbol{\epsilon}-\frac{1}{2}\boldsymbol{\sigma}^T\boldsymbol{S}\ \boldsymbol{\sigma})\,dA - \int_{\partial A_m}\boldsymbol{T}^T(\boldsymbol{u}-\bar{\boldsymbol{u}})\,ds-\int_{S_{\sigma m}}\boldsymbol{T}^{*T}\bar{\boldsymbol{u}}\,ds, \quad (33)$$

where the notations $\boldsymbol{\sigma}$, $\boldsymbol{\epsilon}$, $\boldsymbol{S}$, $\boldsymbol{u}$, $\boldsymbol{T}$ indicate the matrices of the stress, the strain, the compliance, the displacement, and the traction, respectively; for example,

$\boldsymbol{\sigma}^T=[\sigma_{xx}, \sigma_{yy}, \sigma_{zz}, \sigma_{yz}, \sigma_{xz}, \sigma_{xy}]$, and
A_m = area of the m-th hybrid element.
∂A_m : boundary of A_m
$S\sigma_m$: portion of the element boundary where traction is prescribed.
$\boldsymbol{T}^*$: prescribed traction on $S\sigma_m$.
$\bar{\boldsymbol{u}}$: displacement along the element boundary.

Noting that σ_{zz} can be condensed out in terms of the other components, we can rewrite Π_{mh} as

$$\Pi_{mh}(\boldsymbol{\sigma}, \boldsymbol{u}, \bar{\boldsymbol{u}})=\iint_{A_m}(\boldsymbol{\sigma}^T\tilde{\boldsymbol{\epsilon}}-\frac{1}{2}\boldsymbol{\sigma}^T\tilde{\boldsymbol{S}}\boldsymbol{\sigma})\,dA - \int_{\partial A_m}\boldsymbol{T}^T(\boldsymbol{u}-\bar{\boldsymbol{u}})\,ds-\int_{S\sigma_m}\boldsymbol{T}^{*T}\bar{\boldsymbol{u}}ds \quad (34.a)$$

where

$$\boldsymbol{\sigma}^T=\{\sigma_{xx}, \sigma_{yy}, \sigma_{yz}, \sigma_{xz}, \sigma_{xy}\} \quad (34.b)$$
$$\tilde{\boldsymbol{\epsilon}}^T=\{\epsilon_{xx}, \epsilon_{yy}, \gamma_{yz}, \gamma_{xz}, \gamma_{xy}\} \quad (34.c)$$
$\tilde{\boldsymbol{S}}$: the 5×5 matrix of reduced compliance (34.d)

Taking variation of the above functional, we can find that the Euler equations are given by

$$\tilde{\boldsymbol{\epsilon}}=\tilde{\boldsymbol{S}}\boldsymbol{\sigma} \text{ and } \boldsymbol{D}\boldsymbol{\sigma}=0 \text{ in } A_m \quad (35.a)$$
$$\boldsymbol{T}=\boldsymbol{n}\boldsymbol{\sigma} \text{ and } \boldsymbol{u}=\bar{\boldsymbol{u}} \text{ on } \partial A_m \quad (35.b)$$
$$\boldsymbol{T}=\boldsymbol{T}^* \text{ on } S\sigma_m \quad (35.c)$$

where $\boldsymbol{D}$ is the matrix operator for equilibrium equation. We use the asymptotic solution (26.a, b) for $\boldsymbol{\sigma}$ and $\boldsymbol{u}$ and then all of the Euler equations, except for the second in equation (35. b), are satisfied exactly, so that under the traction free condition on $S\sigma_m$ the functional Π_{mh} is reduced to

$$\Pi_{mh}=\int_{\partial A_m}\boldsymbol{T}^T\bar{\boldsymbol{u}}ds-\frac{1}{2}\int_{\partial A_m}\boldsymbol{T}^T\boldsymbol{u}\;ds \quad (36)$$

Equation (26.a, b) may be written in the matrix forms

$$\boldsymbol{\sigma}=\boldsymbol{P}\;\boldsymbol{\beta},\; \boldsymbol{u}=\boldsymbol{U}\;\boldsymbol{\beta}, \quad (37.a, b)$$

and then matrix notation for $\boldsymbol{T}$ can be found from the first of equation (35.b) and the above expression (37.a)

$$\boldsymbol{T}=\boldsymbol{R}\;\boldsymbol{\beta} \quad (37.c)$$

For the displacement along the boundary of hybrid element, we introduce the interpolation

$$\bar{\boldsymbol{u}}=\boldsymbol{L}\;\boldsymbol{q}, \quad (37.d)$$

where $\boldsymbol{q}$ is the nodal degree of freedom common to the hybrid element and the surrounding regular elements. Now the functional Π_{mh} can be written as

$$\Pi_{mh}=\boldsymbol{\beta}^T\;\boldsymbol{G}\;\boldsymbol{q}-\frac{1}{2}\boldsymbol{\beta}^T\;\boldsymbol{H}\;\boldsymbol{\beta}, \quad (38)$$

where

$$\boldsymbol{G}=\int_{\partial A_m}\boldsymbol{R}^T\;\boldsymbol{L}\;ds,\; \boldsymbol{H}=\frac{1}{2}\int_{\partial A_m}(\boldsymbol{R}^T\boldsymbol{U}+\boldsymbol{U}^T\boldsymbol{R})\,ds$$

The stationary property of the first variation of Π_{mh} leads to

$$\boldsymbol{\beta}=\boldsymbol{H}^{-1}\boldsymbol{G}\;\boldsymbol{q} \quad (39)$$

Substitution of equation (39) into (38) yields

$$\Pi_{mh}=\frac{1}{2}\boldsymbol{q}^T\boldsymbol{k}_s\boldsymbol{q},\; \boldsymbol{k}_s=\boldsymbol{G}^T\boldsymbol{H}^{-1}\boldsymbol{G} \quad (40.a, b)$$

where $\boldsymbol{k}_s$ is the element stiffness resulting from the singular hybrid element.

3.2 Formulation of the Regular Elements

For the remaining region surrounding the hybrid element, we use the regular elements based upon the displacement finite element method. In the absence of body forces and tractions, the total potential energy Π_{mp} to be minimized in the problem is given by

$$\Pi_{mp}=\frac{1}{2}\iint_{A_m}\boldsymbol{\epsilon}^T\boldsymbol{C}\boldsymbol{\epsilon}dA, \quad (41)$$

where $\boldsymbol{C}$ is the 6×6 stiffness matrix. Introducing the so-called reduced stiffness matrix defined by

$$\bar{\boldsymbol{C}}=\bar{\boldsymbol{S}}^{-1}$$

we may rewrite Π_{mp} in the reduced from:

$$\Pi_{mp}=\frac{1}{2}\iint_{A_m}\tilde{\boldsymbol{\epsilon}}^T\bar{\boldsymbol{C}}\tilde{\boldsymbol{\epsilon}}dA \quad (42)$$

We now take the standard isoparametric representaion for the displacement components

$$\boldsymbol{u}=\boldsymbol{N}\boldsymbol{q},\; \tilde{\boldsymbol{\epsilon}}=\tilde{\boldsymbol{B}}\boldsymbol{q} \quad (43.a, b)$$

where $\boldsymbol{q}$ is the nodal displacement, and $\boldsymbol{N}$, $\tilde{\boldsymbol{B}}$ are the shape function and the strain matrix, respectively. Substituting this into equation (42), we obtain Π_{mp} in terms of the element stiffness $\boldsymbol{k}_r$

$$\Pi_{mp}=\frac{1}{2}\boldsymbol{q}^T\boldsymbol{k}_r\boldsymbol{q},\; \boldsymbol{k}_r=\iint_{A_m}\tilde{\boldsymbol{B}}^T\bar{\boldsymbol{C}}\tilde{\boldsymbol{B}}dA, \quad (44.a, b)$$

where the subscript "r" indicates the regular elements.

3.3 Solution Procedure

The summation of the two types of element stiffness (40.b) and (44.b) all over the elements will yield the global stiffness $\boldsymbol{K}$, and the global load vector $\boldsymbol{Q}$ may be assembled similarly. Symbolically we may express this assemblage process as

$$\boldsymbol{K}=\boldsymbol{k}_s+\sum_m\boldsymbol{k}_r,\; \boldsymbol{Q}=\boldsymbol{Q}_s+\sum_m\boldsymbol{Q}_r,$$

where m indicate the regular element numbers. The discretized equilibrium equations may be written in the matrix form,

$$\boldsymbol{K}\boldsymbol{q}=\boldsymbol{Q} \quad (45)$$

where the nodal force vector comprises only the reaction vectors at the nodes where displacement components are prescribed, because all tractions are zero throughout the traction boundary conditions. Imposing the displacement boundary conditions among the far-field conditions in Sec. 2. 4, we can solve equation (45) for the unknown nodal displace-

ments and the reaction forces. It is noted that displacement solution is for the composite domain consisting of a singular hybrid element and the displacement based regular elements. The theoretical basis for using such two different variational principles has been treated in Gurtin(1980).

Once the nodal displacements $\boldsymbol{q}$ are obtained, the free constants β_n in the asymptotic representation can be calculated from equation (39), which will complete the solution. As discussed in Ting and Hoang(1984), and Im(1989), the stress does not have the square root singularity for the transverse cracks under consideration and the stress intensity factor as in the linear elastic fracture mechanics of homogeneous materials does not exist. To represent the asymptotic magnification of stress, however, we here use the intensity K_{I}, K_{III} along the crack ligament, and $K_i^{(m)}(i=1\sim6,\ m=1\sim2)$ along the ply interface Im(1989):

$$K_{\mathrm{I}}=\lim_{r\to0} r^{-\delta_s}\sigma_{xx}^{(\alpha)}(r,\phi)$$
$$=\gamma_{31}Re\left[\sum_{k=1}^{2} b_{k1}^{(\alpha)}\mu_k^{(\alpha)}e^{i\phi\delta_s}\right] \tag{46.a}$$

for extension,

$$K_{\mathrm{III}}=\lim_{r\to0} r^{-\delta_s}\sigma_{xz}^{(\alpha)}(r,\phi)=\gamma_{31}Re[b_{11}^{(\alpha)}\xi_1^{(\alpha)}e^{i\phi\delta_s}] \tag{46.a}$$
($\alpha=2,\ \phi=-\pi/2$ for $[90/0]s$, and $\alpha=1$, $\phi=\pi/2$ for $[0/90]s$)

for in-plane shear, (46.b)

$$K_i^{(m)}=\lim_{r\to0} r^{-\delta_s}\sigma_i^{(m)}(r,0)$$
$$=\gamma_{31}Re\left[\sum_{k=1}^{2} b_{k1}^{(m)}\Lambda_{ik}^{(m)}\right]\ (i=1,2,3,6)$$

for extension, (46.c)

$$K_i^{(m)}=\lim_{r\to0} r^{-\delta_s}\sigma_i^{(m)}(r,0)$$
$$=\gamma_{31}Re[b_{i1}^{(m)}\Lambda_{i1}^{(m)}]\ (i=4,5)$$

for in-plane shear, (46.d)

where δ_s is the eigenvalue that characterizes the stress singularity.

4. NUMERICAL RESULT AND DISCUSSION

In this section, we take numerical examples to illustrate the application of the singular hybrid finite element method to the aforementioned two problems. Through the examples, the convergence of numerical solution will be confirmed, and comparison will be made of the results from the present hybrid F.E.M. and those from the boundary collocation technique. Since the nature of the singular field, including the detailed stress distributions, has already been discussed in Im(1989), we here focus upon comparison of the results from the two approaches, and upon discussion of a few points that were not dealt with therein.

Table 1 Eigenvalues

Material A		Material B	
Extension(F)	In-Plane Shear(Ψ)	Extension(F)	In-Plane Shear(Ψ)
−0.34889	−0.54054	−0.35878	−0.5389
0.0	0.54054	0.0	0.5389
0.74718±0.25915i	1.4595	0.79581±0.30952i	1.4610
1.0	2.54054	1.0	2.5389
2.0	3.4595	2.0	3.4610
2.5608 ±1.1318 i	4.5405	2.8296 ±0.92384i	4.5389
3.0		3.0	
4.0		4.0	
4.3379 ±1.7966 i		4.8497 ±1.2212 i	
5.0		5.0	

We use the following two data for numerical examples

material A(Graphite Epoxy)
$E_L=137.9$GPa, $E_T=E_Z=14.5$GPa
$G_{LT}=G_{LZ}=5.86$GPa, $G_{TZ}=3.52$GPa
$\nu_{LT}=\nu_{LZ}=0.21$, $\nu_{TZ}=0.32$

material B(Graphite Epoxy T300/5208)
$E_L=134.45$GPa, $E_T=E_Z=10.20$GPa
$G_{LT}=G_{LZ}=5.52$GPa, $G_{TZ}=3.43$GPa
$\nu_{LT}=\nu_{LZ}=0.3$, $\nu_{TZ}=0.49$

where L, T and Z indicates the fiber, transverse, and thickness directions of each ply, respectively. Material A represents the data that has been suggested to rectify the shortcoming of the material data for graphite epoxy in the earlier literature, for example, Wang and Choi(1982), and Ting and Hoang(1984), where $\nu_{LT}=\nu_{LZ}=\nu_{TZ}$ and $G_{LZ}=G_{LT}=G_{TZ}$ was used(so that the fiber orientation was not taken into consideration in assessing Poisson's ratio and the shear modulus). Material data B has been used for T300/5280(Whitcomb, 1987). Table 1 shows the first thirteen and six eigenvalues for extension and for in-plane shear of the two materials, respectively. In general, there are three eigenvalues associat-

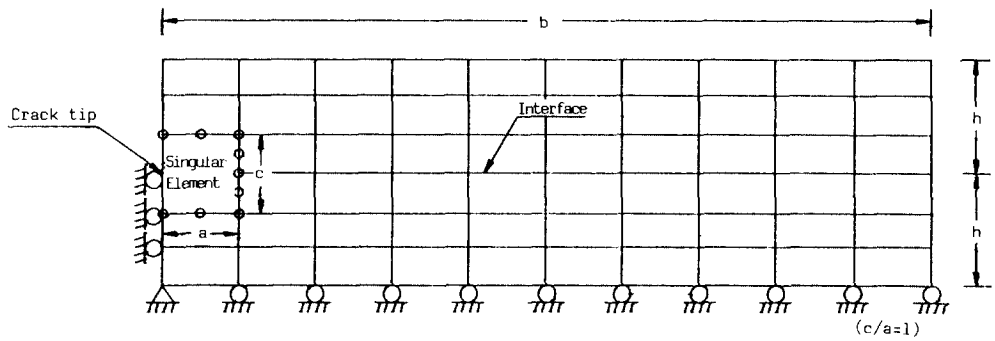

Fig. 2 Typical finite element mesh(the case of 59 elements)

ed with singularity for transverse cracks normal to the ply interface(Ting and Hoang, 1984 ; Im, 1989) : the remaining one that does not appear in Table 1 related to the rotationally antisymmetric deformation associated with F(Im, 1989). This mode has been excluded in the present case by the near-field conditions (11.a). It is note that the in-plane shear involves the stress singularity stronger than the inverse square root singularity of linear homogeneous elastic materials, on the other hand the extension involves the singularity weaker than $r^{-1/2}$. This signifies that the behaviors of crack under these two modes of deformation will be quite different from each other when the transverse crack begins to kink into the interface crack along the ply interface. Under the in-plane shear, the stress intensity of the kinked crack will approach infinity as the size of the kinked crack goes to zero while the limiting value of the stress intensity for the vanishing kinked crack approaches zero under extension(Kim, 1989). Therefore, kinking of the transverse crack into the interface crack is much easier to occur under the in-plane shear rather than under the extension.

A typical finite element mesh is shown in Fig. 2, wherein the region is discretized into 6 by 10 regular 8 node-isoparametric elements through half the thickness ($-h \le y \le h$) and along the x direction ($0 \le x \le b$), except for the crack tip region covered by one singular hybrid element that are two times as large as the regular element (Thus the total number of elements are : $6 \times 10 - 1 = 59$). The convergence of the singular hybrid F.E.M. with the number of elements is shown in terms of K_i in Table 2 and Table 3, and the numerical results obtained by the boundary collocation technique are also tabulated for comparison. The case of 39 elements in the total number of elements has the mesh configuration of $(4 \times 10 - 1)$ element discretization along half the thickness ($-h \le y \le h$) and along the x direction ($0 \le x \le b$), and the case of 127 elements means $(8 \times 16 - 1)$ element discretization : in either case the crack tip region that would be covered by two regular elements is replaced by one singular hybrid element as in Fig. 2. It is noticed that virtually the same results are obtained regardless of the number of elements, and they are in good agreement with the result from the boundary collocation method. The nominal strains ϵ_0 and γ_0 which have been used to normalize K_i in Tables are defined as $\epsilon_0 = u_0/b$ and $\gamma_0 = w_0/b$, where u_0 and w_0 are displacements imposed at $x = b$ when $x = 0$ is fixed.

The stress intensities along the ply interface, $K_i (i = 1 \sim 6)$ for both of $[0/90]_s$ and $[90/0]_s$ under extension were discussed in Im(1989). The stress intensities along the ligament direction, K_I and K_{III} are tabulated for varying values of b/h with h being held constant in Table 4. As b/h increases, the crack density decreases and the stiffness reduction becomes smaller. Noting that the reaction force due to a given nominal strain u_0/b will be proportional to the laminate stiffness, we see that the stress intensity increases at a fixed nominal strain as b/h increases. The stiffness reduction may be considered from the present hybrid finite element analysis, but just regular F.E.M. model as in Lim and Hong(1989) will give enough accurate results as far as only the stiffness reduction is concerned, because it is a global structural property. Stiffness reduction is therefore not considered in the present work. In Table 4, the stress intensities K_I under extension are greater for $[0/90]_s$ than for $[90/0]_s$. This may be expected because the cracked 90° plies in $[0/90]_s$ are constrained by the stiffer 0° plies on the top and bottom while the cracked 90° plies in $[90/0]_s$ are only constrained from the inside and the cracks meet the free surface on the top and bottom. That is, the laminate $[0/90]_s$ is subjected to stiffer constraint that $[90/0]_s$ in the presence of transverse cracks, and the cracked $[0/90]_s$ will therefore show the stiffer sturctural behavior under the same crack density, which leads to greater reaction force at a given nominal strain u_0/b. However this is not the

Table 2 Convergence of solution for extension(Material A, $[0°/90°]_s$) $b/h = 5.535$ $\delta_1 = -0.348895$ unit = GPa(m)$^{-\delta_1}$

Numerical methods	No. of elements (Hybrid F.E.M.) or No. of Collocation stations (Boundary Collocation)	No. of Eigenvalues	K_2/ϵ_0	K_6/ϵ_0
Hybrid F.E.M	39	13	2.0160	−0.98838
	59	13	2.0174	−0.98903
	127	13	2.0178	−0.98926
Boundary collocation method	74	38	2.0120	−0.98643
	96	38	2.0120	−0.98644
	180	38	2.0120	−0.98646
	74	54	2.0153	−0.98805
	96	54	2.0149	−0.98784
	180	54	2.0147	−0.98777

Table 3 Convergence of the solution for in-plane shear (Material B, $[0°/90°]_s$ and $[90°/0°]_s$) $\delta_1 = -0.538912$ $b/h = 5.535$ unit : GPa(m)$^{-\delta_1}$

Nemerical methods	No. of Elements (Hybrid F.E.M.) or No. of Collocation Stations (Boundary Collocation)	No. of Eigenvalues	K_4/γ_0	K_5/γ_0
Hybrid F.E.M.	39	6	0.24610	0.27819
	59	6	0.24623	0.27843
	127	6	0.24619	0.27829
Boundary collocation method	74	18	0.24603	0.27811
	96	18	0.24603	0.27811
	180	18	0.24603	0.27811
	74	27	0.24604	0.27812
	96	27	0.24604	0.27812
	180	27	0.240604	0.27812

Table 4 Stress intensities versus b/h(Meterial B) K_I : GPa(m)$^{0.358781}$ K_{III} : GPa(m)$^{0.538912}$

b/h	$[90°/0°]_s$		$[0°/90°]_s$	
	K_I/ϵ_0	K_{III}/γ_0	K_I/ϵ_0	K_{III}/γ_0
3.690	6.0623	0.31472	6.8655	0.31472
5.535	6.1179	0.36809	6.9793	0.36809
7.380	6.1367	0.37539	7.0137	0.37539
9.225	6.1376	0.37990	7.0449	0.38297
11.07	6.1616	0.38297	7.0325	0.37990
14.76	6.1745	0.38689	7.0606	0.38689

case for the in-plane shear as shown in Table 4. The stress intensities are not dependent upon the lamination sequence under in-plane shear. This is consistent with the fact that the in-plane shear response is dependent only upon the in-plane shear stress component in orthotropic materials, and both 0° and the 90° plies have the same compliance component S_{55}. This is the reason the values of K_4 and K_5 are the same for both of $[0/90]_s$ and $[90/0]_s$ in Table 3.

5. CONCLUSION

Stress field near transverse cracks in cross-ply laminates has been examined for extension and in-plane shear by use of Leknitskii's complex-potentials and the singular hybrid finite element method. We may summarize the conclusion of the present study as follows:

(1) The in-plane shear case has the stress singularity stronger than $r^{-1/2}$, and thus greater tendency that the transverse cracks kink into the delamintion cracks, compared with the case of extension wherein the stress singularity is weaker than the inverse square root singularity.

(2) In terms of the stress intensity factors, the numerical results from the present singular hybrid F.E.M. is in excellent agreement with those form the boundary collocation technique Im(1989), reported earlier.

(3) Under in-plane shear, the cross-ply laminate, $[90/0]_s$ and $[0/90]_s$ show the same response—the response is independent of the lamination sequence—because S_{55} is invariant under 90° rotation, while the response under extension is depedent upon the lamination sequence.

REFERENCE

Bogy, D.B., 1971, "On the Plane Elastostatic Problem of a Loaded Crack Terminating at a Material Interface", J. Appl. Mech., Vol. 38, pp. 911~918.

Cook, T.S and Erdogan, F., 1972, "Stresses in Bonded Materials with a Crack Perpendicular to the Interface", J. Engng. Sci., Vol. 10, pp. 677~679.

Gurtin, M.E., 1980, "On Patched Variational Principles in Elasticity", J. Elasticity, Vol. 10, pp. 329~332.

Im, S., 1989, "Asymptotic Stress Field Around a Crack Normal to the Ply-Interface of an Anisotropic Composite Laminate", To appear in Int. J. Solids Structures.

Kim., H.J., 1989, "Stress Distribution Around Delamination Cracks Kinked from Transverse Cracks in $[90/0]_s$ Composite Laminates", M.S. Thesis, Korea Advanced Institute of Science and Technology.

Lekhnitskii, S.G., 1963, "Theory of Elasticity in an Anisotropic Body", Holden-Day, San Francisco

Lim, S.K and Hong, C.S., 1989, "Effect of Transverse Cracks on the Thermomechanical Properties of Cross-Ply Laminated Composites", Composite Sci. Tech., Vol. 35, pp. 145~162.

Ting, T.C.T and Chou, S.C. 1981, "Edge Singularities in Anisotropic Composites", Int. J. Solids Structures, Vol. 17, pp. 1057~1068.

Ting, T.C.T and Hong, P.H., 1984, "Singularities at the Tip of a Crack Normal to the Interface of an Anisotropic Layered Composite", Int. J. Solids Structures, Vol. 20, pp. 430~454.

Wang, S.S., 1984, "Edge Delamination in Angle-Ply Composite Laminates", AIAA Journal, Vol. 22, pp. 256~264.

Wang, S.S., and Choi, I., 1982, "Boundary-Layer Effect in Composite Laminates. Part I-Free-Edge Stress Singularities: Part Ⅱ-Free-Edge Stress Solutions and Characteristics", J. Appl. Mech, Vol. 49, pp. 541~550.

Wang, S.S and Choi, I., 1983, "The Mechanics of Delamination in Fiber Composite Materials", Part Ⅰ-Stress Singularities, NASA-CR-172269, National Aeronautics and Space Administration-Langley Research Center, Hampton, VA.

Wang, S.S and Yuan, F.G., 1983, "A Hybrid Finite Element Approach to Compotite Laminate Elasticity Problems with Singularites", J. Appl. Mech, Vol. 50, pp. 835~844.

Washizu, K., 1982, "Variational Methods in Elasticity and Plasticity", 3rd Edition, Pergamon Press, Oxford, England, pp. 439~440.

Whitcomb, J.D., 1987, "Three Dimensional Analysis of a Postbuckled Embedded Delamination", Mech. of Comp. Review, edited by D.C. Mueller, pp. 88~98.

Zak, A.R and Willams, M.L., 1963, "Crack Point Stress Singularities at a Bi-Material Interface", J. Appl. Mech., Vol. 30, pp. 142~143.